Molecular Human Reproduction, Vol.17, No.11 pp. 669–678, 2011
Advanced Access publication on May 18, 2011 doi:10.1093/molehr/gar037

MHR Basic science of reproductive medicine

ORIGINAL RESEARCH

Highly purified spermatozoal RNA obtained by a novel method indicates an unusual 28S/18S rRNA ratio and suggests impaired ribosome assembly

Heike Cappallo-Obermann [1], Wolfgang Schulze [1], Holger Jastrow [2], Vera Baukloh [3], and Andrej-Nikolai Spiess [1,*]

[1]Department of Andrology, University Hospital Hamburg-Eppendorf, Martinistr. 52, 20246 Hamburg, Germany [2]Institute of Anatomy, University of Duisburg-Essen, Essen, Germany [3]Fertility Center Hamburg FCH, Hamburg, Germany

*Correspondence address. Tel: +49-40-7410-51585; Fax: +49-40-7410-51554; E-mail: a.spiess@uke.de

Submitted on March 25, 2011; resubmitted on May 4, 2011; accepted on May 9, 2011

ABSTRACT: Human spermatozoal RNA features special characteristics such as a significantly reduced quantity within spermatozoa compared with somatic cells is described as being devoid of ribosomal RNAs and is difficult to isolate due to a massive excess of genomic DNA in the lysates. Using a novel two-round column-based protocol for human ejaculates delivering highly purified spermatozoal RNA, we uncovered a heterogeneous, but specific banding pattern in microelectrophoresis with 28S ribosomal RNA being indicative for the amount of round cell contamination. Ejaculates with different round cell quantities and density-purified spermatozoa revealed that 18S rRNA but not 28S rRNA is inherent to a pure spermatozoal fraction. Transmission electron microscopy showed monoribosomes and polyribosomes in spermatozoal cytoplasm, while immunohistochemical results suggest the presence of proteins from small and large ribosomal subunits in retained spermatozoal cytoplasm irrespective of 28S rRNA absence.

Key words: human spermatozoa / RNA isolation / ejaculate / electropherogram / Bioanalyzer / 18S/28S rRNA ratio

Introduction

Human spermatogenesis is a highly specialized process, starting from spermatogonia and resulting in spermatozoa after a multitude of differentiation steps that include haploidization and significant morphological changes such as the loss of cytoplasm and acrosome/flagellum formation. In order to deliver paternal DNA to the oocyte, the majority of histones are exchanged by smaller protamines to achieve nuclear compaction (Miller *et al.*, 2010). However, the important role of spermatozoal DNA transcripts has recently been extended with reports that highlight the importance of spermatozoal RNA in sperm function, maintenance and fertilization.

Transcriptional activity during spermatogenesis is high in primary spermatocytes, decreases during progression of meiosis, exhibits another surge during spermatid development and is then continuously shut down in spermiogenesis to allow chromatin repackaging (Dadoune *et al.*, 2004). Although the RNA load of mature spermatozoa can be largely regarded as the result from its testicular history, differences can exist between subgroups of spermatozoa, such as motile compared with non-motile (Lambard *et al.*, 2003; Steger *et al.*, 2003). The subcellular localization of RNA can exhibit a heterogeneous pattern, such as in the mid- and principle piece of tail (Kumar *et al.*, 1993) or in the sperm head (Pessot *et al.*, 1989; Wykes *et al.*, 1997; Dadoune *et al.*, 2005), often accumulating at high concentrations in the nuclear periphery (Lalancette *et al.*, 2009). Therefore, it has been postulated that spermatozoal RNA might be trapped in or around the condensing nucleus (Miller *et al.*, 2005).

Using an *in vitro* model with radio-labeled UTPs, it was demonstrated that spermatozoa lack intrinsic transcriptional activity (Grunewald *et al.*, 2005). In contrast to this, spermatozoa can reverse transcribe exogenous RNA into cDNA (Giordano *et al.*, 2000) and retain an inducible molecular machinery to transcribe exogenous DNA into RNA, remove intronic sequences, splice the transcript and convert it to cDNA (Pittoggi *et al.*, 2006). Another investigation showed that capacitating spermatozoa can synthesize polypeptides from fluorophore-labeled amino acids, as visualized by autoradiography and fluorescence microscopy. An interesting aspect of this study was that mitochondrial but not cytoplasmic translation inhibitors abolished polypeptide synthesis completely, suggesting that nuclear encoded transcripts are translated on mitochondrial ribosomes (Gur and Breitbart, 2006).

Considering that spermotozoal RNAs are generally accepted as being remnants of spermatogenesis (Miller et al., 1999; Ostermeier et al., 2002), novel findings with respect to RNA exchange during fertilization contradict the marginal role of spermatozoal RNA. Several mRNAs are delivered to the oocyte by the spermatozoon, as elegantly shown by a hamster oocyte penetration model (Ostermeier et al., 2004). Spermatozoal transcripts such as the pregnancy-specific β-1-glycoprotein and human leukocyte antigen-E are even detectable 24 h after oocyte penetration (Avendano et al., 2009). A recent study has also revealed the important role of spermatozoal RNA in conferring non-Mendelian inheritance by reverting the phenotype of a Kit tyrosine kinase receptor knockout by means of *Kit* mRNA microinjection into oocytes (Rassoulzadegan et al., 2007).

In the last years, increasing interest has emerged in the investigation of spermatozoal transcript levels on a global scale using microarray technology. This has contributed further to the understanding of mRNA complexity in these cells, giving rise to the identification of specific mRNA patterns that correlate with male fertility/infertility (Wang et al., 2004; Ostermeier et al., 2005; Garrido et al., 2009; Lalancette et al., 2009; Garcia-Herrero et al., 2010), sperm morphology/motility (Lambard et al., 2004; Platts et al., 2007), smoking (Linschooten et al., 2009) and cryptorchism effects (Nguyen et al., 2009).

Therefore, the development of isolation methods that deliver highly purified and intact spermatozoal RNA for downstream applications such as microarray profiling or PCR is of interest. However, for spermatozoal RNAs some essential problems exist such as a significantly different DNA:RNA ratio compared with somatic cells, with only 10–50 fg RNA estimated per spermatozoon (Krawetz, 2005; Miller et al., 2005), and the absence of ribosomal RNA (rRNA) for stringent control of potential RNA degradation (Miller et al., 1999; Ostermeier et al., 2002; Grunewald et al., 2005; Miller et al., 2005). Interestingly, results with respect to the latter are conflicting (Betlach and Erickson, 1976; Gur and Breitbart, 2006) and might depend strongly on the extraction method (Gilbert et al., 2007).

In the present study we developed a spermatozoal RNA extraction protocol which is independent of DNase I digestion, as commercial formulations of DNase I are not guaranteed to be free of residual RNase activity and must be tested individually (Goodrich et al., 2007). Based on highly purified RNA obtained with this new method, we aimed to clarify if the absence of rRNA and/or ribosomal subunits is a general characteristic of human spermatozoa and if there are distinct or common features within high-resolution microelectrophoretic patterns of spermatozoal RNA isolated in the presence/absence of somatic cells.

Materials and Methods

Human semen samples

Fresh semen samples were collected from patients of the Department of Andrology, University Hospital Hambug-Eppendorf, Germany ($n = 33$, prefixed with 'Sp') and of the Fertility Center Hamburg GmbH, Germany ($n = 32$, prefixed with 'F'). Testicular biopsies ($n = 22$) were obtained from a previous study (Feig et al., 2007). Informed consent and ethic committee approval was obtained (OB/X/2000) and the study was conducted in accordance with the guidelines of the 'Helsinki Declaration'. Spermatozoal parameters were analyzed according to the World Health Organization 1999 guidelines. An estimate for contamination with round cells for samples from the Department of Andrology was acquired as follows. First, the ejaculate was inspected by bright-field microscopy. Samples exhibiting a high proportion of round cells were investigated with a MultiStix™ (Siemens Healthcare, Eschborn, Germany) dipstick with respect to an increased proportion of erythrocytes or leukocytes. If this was the case (by intense staining), samples were classified qualitatively for leukocytes, epithelial cells or round germ cells by differential staining (Testsimplets®, Waldeck, Germany). Results of all ejaculate parameters are given in Supplementary data S2.

Purification of spermatozoa

In case of density gradient purification, 1 ml of liquefied ejaculate was pipetted on top of a discontinuous gradient consisting of 3 ml 40% and 3 ml 80% SpermFilter (Cryos, Aarhus, Denmark). After centrifugation (538*g*, 20 min, 4°C) three fractions (F1: ejaculate/40% interphase; F2: 40%/80% interphase; and F3: 80% bottom pellet) were collected. Successful purification from round cells was checked by methylene blue staining and light microscopy. Each of the fractions was washed with 15 ml 1× PBS buffer, pelleted by centrifugation (800*g*, 5 min, 4°C) and frozen at −80°C until RNA purification.

RNA isolation

After liquefaction, 1 ml of ejaculate was washed with 50 ml 1× PBS. Cells were pelleted by centrifugation (500*g*, 15 min, 4°C) and frozen at −80°C. Total RNA was isolated by the RNeasy Plus Micro Kit (Qiagen, Hilden, Germany) according to the instructions of the manufacturer. Briefly, frozen cell pellets were immediately suspended in RLT Plus Lysis buffer in the presence of 10 mM β-mercaptoethanol (1.2 ml/2 × 10^7 spermatozoa). Homogenization was conducted using an Ultra-Turrax™ for 30 s. The lysate was divided into aliquots corresponding to maximally 2 × 10^7 spermatozoa. Two aliquots were directly used for RNA isolation, using one set of columns for each aliquot and the remaining aliquots were frozen at −80°C for later RNA isolation. Genomic DNA was eliminated from the RNA lysate by DNA-binding spin columns (gDNA columns), and the flowthrough bound to RNA Microextraction spin columns that efficiently bind even minor amounts of RNA (lower size cutoff ∼100 nt). After on-column washing steps, the RNA was eluted with 20 µl RNAse free water. The two RNA aliquots from the same sample were combined and purified from residual contamination with genomic DNA by (i) a second round with the above procedure or by (ii) digestion with DNase I (Sigma-Aldrich, Hamburg, Germany) according to the supplier's protocol for 15 min at ambient temperature. Purified RNA was stored at −80°C. The complete workflow of this procedure is summarized in Supplementary data S1. Total RNA from testicular biopsies was isolated as described in Feig et al. (2007).

Analysis of RNA electrophoresis pattern and concentration

Total RNA was checked by analyzing 1 µl RNA by on-chip gel electrophoresis on a Bioanalyzer 2100 instrument (Agilent, Waldbronn, Germany) using the RNA 6000 Pico Kit. Electropherograms of different runs were aligned by the 'Comparison function' of the Bioanalyzer Expert software (Revision B.02.06). All peak (18S/28S rRNA) areas were quantified from the trace data with the *R*-script 'peak area' using Simpson's rule for numerical integration (www.dr-spiess.de/Rscripts.html). For better visual display, electropherograms were normalized to the height of the 18S rRNA peaks. RNA concentration was determined by optical UV photometry at 260 nm (NanoDrop ND-1000, Thermo Scientific, Germany).

Detection of genomic DNA

Contamination of RNA with genomic DNA (gDNA) was analyzed by PCR with intron-spanning primers for protamine 1 (PRM1; forward primer: tcacagcccacagagttcca; reverse primer: aggcaggagtttggtggatg) using ExTaq™ HS DNA Polymerase (Takara Bio, Saint-Germain-en-Laye, France). Two microliters of 10× ExTaq™ buffer was mixed with 2 µl of dNTP mixture (2.5 mM each), 500 nM of primers each, 4 U ExTaq™ HS DNA Polymerase, 2 µl of RNA (diluted 1:10 with H_2O) and H_2O to a total volume of 20 µl in a 0.2 ml PCR tube. Amplification was done in a thermal cycler (Cyclone Gradient, Peqlab, Erlangen, Germany) with the following cycling program: 98°C 10 s, 60°C 30 s and 72°C 30 s with 30 cycles, followed by a final extension step at 72°C for 5 min. One microliter of the PCR reaction was analyzed on a Bioanalyzer 2100 (DNA 1000 Chip). Amplicon length was 285 bp for cDNA and 376 bp for genomic DNA.

Quantitative real-time PCR of 18S and 28S ribosomal RNA

The complete RNA from density gradient-purified spermatozoa was heat denatured (65°C, 5 min) in a total volume of 9.4 µl after adding 1 µl 10 mM dNTP and 1.6 µl random hexamers (250 ng/µl). After cooling on ice, 4 µl 5× First Strand Buffer/2 µl 100 mM DTT/1 µl RNAse Block/1 µl Superscript II (Invitrogen, Karlsbad, USA) were added to a final volume of 20 µl and reverse transcription conducted at 25°C 10 min, 42°C 50 min and 70°C 15 min.

cDNA was amplified in a Lightcycler 1.0 instrument (Roche, Basel) using a Sybr ExTaq II-Premix (Takara Bio, Saint-Gemain-en-Laye, France) and 8 pmol each of 18S specific primers (sense: AGTGTTCAAAGC AGGCCCGA, antisense: GCTTTCGCTCTGGT-CCGTCT; GeneBank NR_003286.2; product size: 183 bp) or 28S (sense: TCCTTCTGATC GAGGCCCAG, antisense: GGACCCCACCCGTTTACCTC; GeneBank NR_003287.2; product size: 248 bp) with the following program: 95°C 10 s/30 cycles of 95°C 5 s, 61°C (18S) or 63°C (28S) 30 s. Specificity of the products was evaluated by melting point analysis, appropriate amplicon size (Bioanalyzer) and sequencing. 28S/18S rRNA ratios were calculated by the ΔΔct method using individual quantitative real-time PCR (qPCR) efficiencies (Pfaffl, 2001).

Transmission electron microscopy of spermatozoa

An ejaculate of a fertile 43-year old donor was immediately fixed in glutaraldehyde solution (2.5% in 0.1 M cacodylate buffer, pH 7.4). After fixation for 4 h at room temperature, a centrifugation at 200 *g* for 5 min was performed and the pellet washed in pure cacodylate buffer for 3 × 20 min and then kept in buffer overnight. The following steps were conducted in darkness at room temperature. After 30 min each in 50 and 30% ethanol, the pellet was transferred into a cacodylate buffer solution containing 1% osmium tetroxide for 90 min. Washing in cacodylate buffer for 3 × 20 min was followed by ethanol 30 and 50% (40 min each). Contrast was enhanced by 1% uranyl acetate in 70% ethanol. After 80%, 90% and 96% ethanol (40 min each), pure ethanol was applied 3× for 10 min each followed by 2 × 15 min propylene oxide. The sample was incubated in EPON® solutions (Polysciences, USA) in propylene oxide with increasing concentrations (3:1, 1:1, 1:3; 60 min each) and finally pure EPON® overnight. Embedding was performed in flat embedding wells by polymerization in a heated storage (60°C, 2 days). After trimming, solid EPON® blocks were cut on an ultramicrotome (Reichert-Jung Ultracut®, Vienna, Austria) set to a thickness of 70 nm. Sections were then mounted on 200-mesh hexagonal copper grids and treated with 1% aqueous uranyl acetate solution for 20 min followed by 5 min of lead citrate (0.4% in water) for contrast enhancement. Dried sections were investigated on a Zeiss transmission electron microscope (EM 902A) at 80 kV at magnifications ranging from 3000 to 140 000×. Digital image acquisition was performed on a MegaViewII slow-scan-CCD camera connected to a PC running ITEM® 5.0 software (Soft-imaging-systems, Münster, Germany). Acquired images were stored as uncompressed TIFF files in 16 bits of gray.

Immunohistochemical staining of small and large ribosomal subunits retained in spermatozoal cytoplasm

After liquefaction, human ejaculates were washed in PBS and an aliquot of 2×10^7 spermatozoa was frozen at −80°C for RNA extraction and microelectrophoretic separation. To the washed ejaculate pellet, a 4% fresh paraformaldehyde/PBS solution was added. This procedure, similar to the observations made by Cooper *et al.* (2004), avoids the loss of spermatozoal cytoplasm when ejaculates are smear dried prior to fixation. The ejaculates were fixed for 3 h at 4°C, smeared onto poly-lysine-coated slides and air dried. Cells were permeabilized by incubating slides for 10 min in PBS/0.1% Triton X-100 (Roth, Germany) and subsequent washing for 1 min in PBS. A 1.5 × 1.5 cm area, bordered with Fixogum (Marabu, Germany), was overlayed with 100 µl of primary antibodies (rabbit polyclonal to S10 ribosomal protein, Abcam #ab95994; rabbit polyclonal to L26 ribosomal protein, Abcam #ab59567) at a 1:100 dilution in PBS/0.1% Triton X-100/1% blocking reagent (Roche Biochemicals, Germany) for 48 h at 4°C. Slides were washed in PBS/Triton-X and PBS (5 and 1 min, respectively) and incubated with a horseradish peroxidase-conjugated anti-rabbit polymer (Dako Envision System, Dako, CA, USA) for 3 h at room temperature. After washing as above, cytoplasmic ribosomes were visualized by chromogenic substrate conversion using the Liquid DAB+ Chromogen System (Dako, CA, USA) at 15 min incubation.

Results

Isolation of highly purified RNA from whole human ejaculates

In order to develop a DNase I-free RNA isolation procedure which provides optimal RNA yield together with efficient removal of residual gDNA contamination, we chose a set of ejaculates from three donors (Sp81, Sp84, Sp86; see Supplementary data S2) presenting significantly different sperm concentrations. We performed RNA isolations with the RNeasy Plus Micro Kit according to standard protocols, with elimination of gDNA from the cell lysate by gDNA eliminator columns and subsequent binding of RNA to RNA extraction columns. After two on-column washing steps, RNA was eluted in small volumes of RNAse free water (down to 15 µl). Analysis of RNA fragment patterns by on-chip gel electrophoresis using RNA Pico Chips on a Bioanalyzer 2100 instrument revealed prominent broad bands in a region of 1000–2000 nt (Fig. 1A, lanes 1, 2 and 5). We assumed residual contamination with gDNA as the origin of these bands and confirmed this with the amplification of the genomic PRM1 sequence by PCR using intron-spanning primers (Fig. 1B, lanes 1, 2 and 5). However, after a second-round clean-up of the previously eluted RNA (Supplementary data S1), genomic DNA failed to be detected by PCR after 30 cycles, indicating a highly purified RNA isolate (Fig. 1B, lanes 3 and 4). We investigated the sensitivity cut-off for this PCR validation and were able to detect 144 pg genomic DNA by PCR (data

not shown), which reflects the DNA content of approximately 40 spermatozoa. Since the lysis buffer/genomic DNA columns are from a system for higher cell numbers (RNeasy Mini Kit, Qiagen), there is no danger of lysis buffer overload. RNA overload on the RNeasy columns is also unlikely as the average amount of total RNA isolated from 2×10^7 spermatozoa ($\sim$ 800 ng) is far from the saturation limit of the columns ($\sim$ 45 μg, Qiagen manual).

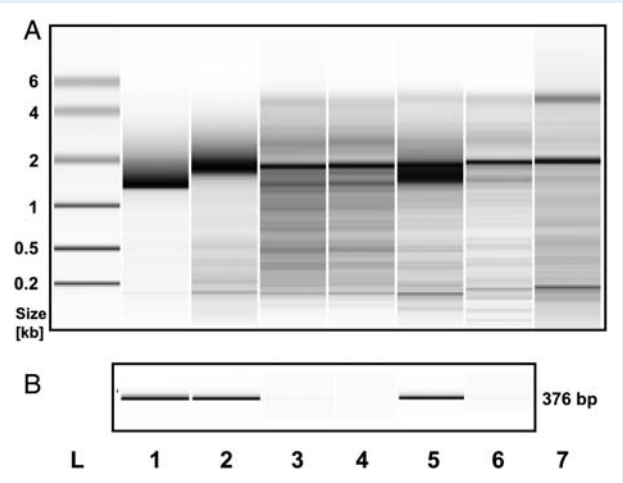

Figure 1 Purification of RNA and removal of residual contaminating gDNA. (**A**) Gel-like representation obtained from Bioanalyzer 2100 RNA electropherograms. (**B**) PCR with intron-spanning primers for PRM1 (size of genomic product: 376 bp). L: RNA size ladder; lanes 1, 2, 5: one round of RNA purification; lanes 3, 4: two rounds of RNA purification; lane 6: one round of purification and additional digestion with DNase I; lane 7: human testicular total RNA.

In order to ensure that the isolated RNA contains mostly spermatozoal RNA, we analyzed the RNA from 25 human ejaculates by microarray hybridization for a study to be published elsewhere (Codelink Human Genome 55 K chips; GEO Accession #29002) with respect to germ cell-specific transcripts. The three germ cell-specific transcripts protamine-2 (PRM2), germ-cell associated 1 (GSG1) and transition protein 1 were detectable in all samples (Supplementary data S3A). Furthermore, from the 20774 transcripts with signal levels above background, PRM2 and GSG1 were always the most abundant transcripts ($\sim$120-fold over background). This demonstrates that germ cell-specific transcripts are commonly and prevalently detected within the RNA pool obtained by the new procedure.

Characteristics of individual RNA capillary electrophoresis patterns

After genomic DNA removal, the prominent bands were replaced by a pattern of distinct RNA fragments in the range from 100 to 4000 nt (Fig. 1A, lanes 3 and 4) with two more intense bands of sizes $\sim$2000 and $\sim$4000 nt. These two bands migrated equal to those of a testis biopsy (Fig. 1A, lane 7), commonly accepted to be 18S and 28S ribosomal RNA. We therefore chose to refer to these bands as 18S rRNA and 28S rRNA in the present study. Similar results to our two-round clean-up procedure were obtained by the digestion of residual gDNA in the samples with DNAse I (Fig. 1A and B, lane 6).

To refine the investigation of RNA variability, we expanded our study to a large cohort of ejaculates ($n = 32$) collected at the Fertility Center Hamburg. Sperm parameters tested in pre-examinations were

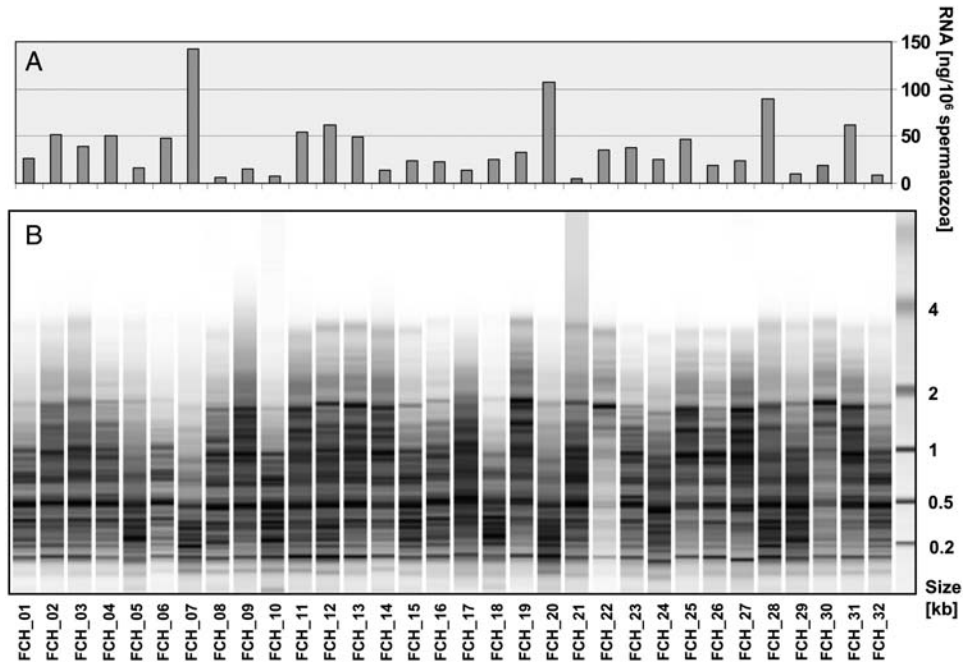

Figure 2 RNA isolation and analysis of ejaculates from 32 patients. (**A**) RNA yield from 10^6 spermatozoa. (**B**) Electropherograms (RNA 6000 Pico Chip) of the same RNAs. Note the heterogeneity of the profiles as well as the similarity of some banding patterns.

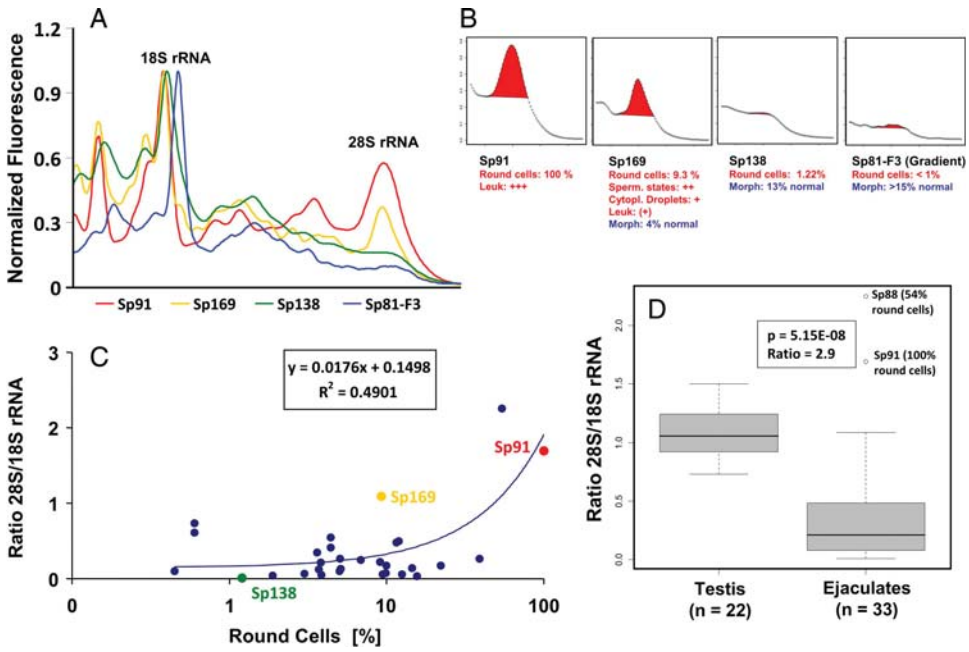

Figure 3 Analysis of 28S rRNA peaks in dependence of sperm purity and round cell quantity. (**A**) Microelectrophoretic traces of four RNAs from ejaculates with decreasing amounts of round cells. Trace data are 18S rRNA normalized to visualize the differences in 28S rRNA quantity. (**B**) Magnified 28S rRNA peaks/areas and ejaculate parameters from the four samples in (A). Sp91 is azoospermic and features 100% round cells, with a high proportion of leukocytes. Sp169 has ~10% round cells, mostly spermatogenic states and low leukocyte quantity. Sp138 has ~1% round cells and good morphology. Sp81-F3 is a highly pure F3 percoll fraction with <1% round cells and very good morphology. (**C**) Linear regression of 28S/18S rRNA ratio in dependence of round cell quantity shows good correlation between these two parameters. X-axis in logarithmic scale. (**D**) Comparison of 28S/18S rRNA ratios obtained from 22 testicular RNA samples and 33 ejaculate RNA samples. Ratios are highly significantly different ($P = 5.15E-8$), with the ratio in testis being 2.9× higher than in ejaculates.

normal according to WHO guidelines (1999), including the concentration of leukocytes which did not exceed 10^6/ml. The RNA yield obtained with our protocol was within a broad range from 5 to 143 ng/10^6 spermatozoa with an average of 37 ng (Fig. 2A). RNA patterns were highly heterogeneous, with expression strengths of single peaks varying from donor to donor as well as differences in the relative number of bands in each donor, therefore providing individual RNA 'fingerprints' (Fig. 2B, FCH_01 – FCH_32). Despite the overall heterogeneity, many samples exhibited prominent bands with sizes ~500, 1000 and ~1900 nt (18S rRNA). In contrast, the 28S rRNA band (~3800 nt) displayed a high variability in its intensity through all samples. To exclude differences in microelectrophoretic profiles as a consequence of technical variation in the isolation or electrophoresis, we ran the same RNA multiple times on a chip and also included two RNAs isolated individually from the same sample (Supplementary data S3B). The microelectrophoretic profiles displayed a high concordance within the replicates, demonstrating that individual profiles are sample and not procedure specific.

Effect of round cell content on RNA profiles

We concluded by these results that spermatozoal RNA needs to be highly purified in order to uncover its specific banding pattern in high-resolution capillary electrophoresis. Since the presence of round cells (somatic cells like epithelial cells/leukocytes or round spermatogenesis cell types such as round spermatids/primary spermatocytes) should alter the RNA banding pattern, we next investigated the influence of round cell contamination on the RNA electropherograms. For this purpose, we selected three ejaculates with 100% (azoospermic), 9.3 and 1.2% round cells (Sp91, Sp169, Sp138; see Supplementary data S2), and a F3 gradient centrifugation fraction (Sp81-F3) with less than 1% round cells for electrophoretic separation. We focused on 28S rRNA quantity, which was significantly different between these samples (Fig. 3A), by calculating the 28S/18S rRNA ratios based on their peak areas, as exemplified for the 28S rRNA peaks in Fig. 3B. Using a larger cohort of ejaculate samples with differing round cell contents, linear regression analysis showed a clear correlation between 28S/18S rRNA ratio and round cell quantity (Fig. 3C). Finally, a comparison between testis and ejaculate 28S/18S rRNA ratios showed a highly significant ($P = 5.15E-8$) difference in ratios when a somatic compartment is present (Fig. 3D).

To further corroborate the findings in respect to 28S rRNA quantity, we fractionated two samples containing 7 and 10% round cells (Sp81 and Sp83; see Supplementary data S2) into different round cell quantities by discontinuous density gradient centrifugation. By checking harvested cell fractions with light microscopy, we observed the usual accumulation of round cells on the ejaculate/40% layer interphase (F1). The fraction collected from the 40%/80% interphase (F2) was devoid from round cells, while the pellet from the bottom of the 80% phase (F3) consisted exclusively of spermatozoa. 18S rRNA

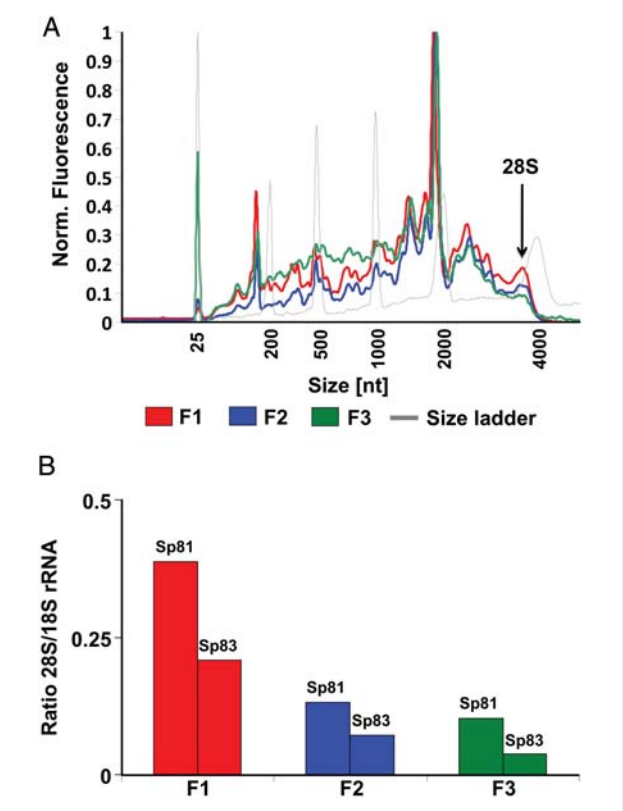

Figure 4 Decrease of 28S/18S rRNA ratio with increasing purity of the spermatozoal fraction. (**A**) RNA electropherograms (normalized to 18S rRNA signal) from a human ejaculate (Sp83, 10.2% round cells) after density gradient centrifugation. F1: Ejaculate/40% SpermFilter™ interphase; F2: 40%/80% SpermFilter™ interphase and F3: 80% SpermFilter™ pellet. The F3 fraction was essentially free of round cells as examined by methylene blue staining and bright-field microscopy. (**B**) Calculated 28S/18S rRNA ratios of two ejaculates with increasing purity in the F1–F3 fractions after density gradient centrifugation.

peak-normalized electropherograms from the three fractions, as exemplified for Sp83, are shown as overlays in Fig. 4A. Similar to the findings described in Fig. 3C, the 28S rRNA peak (Fig. 4A, arrow) correlated highly with the round cell content of the fractions, resulting in the reduction of 28S/18S rRNA ratios from F1 to F3 (Fig. 4B). The electrophoretic profile in Fig. 4A also highlights an interesting observation concerning the general banding pattern of spermatozoal RNA: while the intensity of the ribosomal bands (especially the 28S rRNA) depends on the round cell proportion of the ejaculate, a high degree in profile concordance is observed within the lower intensity peaks in the three fractions (regions 200–1500 and 2200–3000 nt), even though the relative expression levels (magnitude of profiles) underly individual fluctuations.

We finally evaluated the presence of 18S and 28S rRNA in spermatozoa by using qPCR of density gradient-purified spermatozoa using rRNA-specific primers. This has the advantage of not only detecting the presence of rRNA but also of accurately quantifying the 28S/18S ratio. 28S as well as 18S rRNA transcripts were present in considerable amounts in five different fractions (Supplementary data S4A). The qPCR products were highly specific, as controlled by amplicon size (Supplementary data S4B) and sequencing. Calculation of 28S/18S rRNA ratios in this pure spermatozoal fraction using the $\Delta\Delta$ct method indicates a significantly lower ratio (median = 0.11) than what is commonly described for somatic cells (~1.5–2) or an assumed 1:1 equimolar ratio in ribosomes.

Investigation of structures in the cytoplasm of spermatozoa by transmission electron microscopy

As our findings indicated the presence of 28 s rRNA-depleted ribosomes in spermatozoa, we investigated the ultrastructure of spermatozoal cytoplasm with respect to the presence of ribosomes. TEM at 3000–24000× revealed highly electron-dense irregularly bordered profiles (20–25 nm in diameter) in the cytoplasm of the neck to beginning of midpiece region in over 25% of all spermatozoa that were cut in the relevant area (Fig. 5A1 and 5B1). These profiles corresponded exactly to clearly identifiable ribosomes on the rough endoplasmic reticulum (rER) of other cells contained in the same specimen (data not shown). It can thus be concluded that the singly lying profiles derived from monoribosomes (Fig. 5B2) were similar to those appearing in rows, belonging to polyribosomes or remnants of sheared rER (Fig. 5A2).

Immunohistochemical investigation of small and large ribosomal subunits in the cytoplasm of spermatozoa from different ejaculates

The absence of 28S rRNA could be an indication for a disturbed assembly of the large ribosomal subunit. We therefore inspected by immunohistochemical staining against the small ribosomal subunit protein RPS10 and the large ribosomal subunit protein RPL26, if there are differences with respect to subunit quantity in the spermatozoal cytoplasm (Fig. 6). Four different ejaculates featuring different characteristics (Sp183: 2% round cells, good morphology, hyperspermia; Sp185: 22% round cells, teratozoospermic; Sp186: 5% round cells, good morphology; Sp190: 4% round cells, good morphology) were fixed in 4% paraformaldehyde prior to slide spreading in order to avoid dehydration and removal of spermatozoal cytoplasm while drying (Cooper *et al.*, 2004). In all four ejaculates, intense staining for both ribosomal proteins could be observed in round cells as well as significantly smaller and circular bodies, most probably cytoplasmic remnants, with a few exceptions. In general, intense staining was also observed in spermatozoa with increased cytoplasm in the head/neck region, while morphological intact spermatozoa lacked any staining. In the presence of increased cytoplasm, staining could differ substantially with respect to spermatozoal origin: in some ejaculates with substantially higher percentages of normal forms (Sp183, Sp190), morphological aberrant spermatozoa were found that lacked any signals, while in other ejaculates (Sp185, Sp186), increased spermatozoal cytoplasm was clearly associated with intense staining against both ribosomal proteins. A teratozoospermic sample (Sp178) served as a primary and secondary antibody control with negative staining.

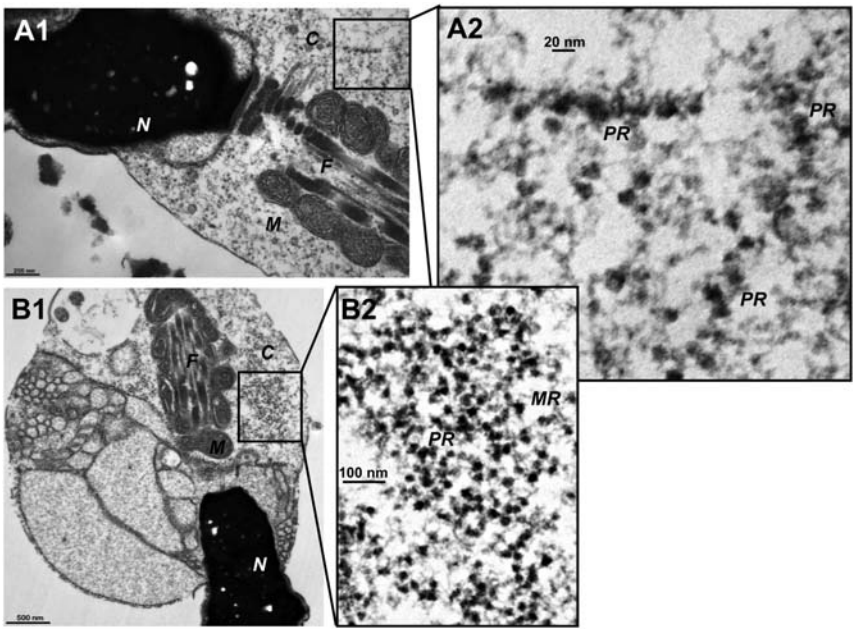

Figure 5 Transmission electron micrographs of human spermatozoa showing irregularly bordered small highly electron-dense profiles (most probably ribosomes) within the cytoplasmic compartment. (**A1**) Longitudinal section through head/neck region showing the nucleus (*N*), mitochondria (*M*), axial filaments (*F*) and cytoplasm (*C*). (**A2**) Details of the cytoplasmic region showing polyribosomes (PR). (**B1**) Transversal section through head. (**B2**) Enlargement of an area with many profiles of monoribosomes (MR) and polyribosomes (PR). The scale bars indicate the different magnifications.

Discussion

Increased attention has been drawn to the analysis and characterization of human spermatozoal RNAs since the hallmark descriptions of complex mRNA patterns in human spermatozoa (Miller *et al.*, 1999; Ostermeier *et al.*, 2002). These initial findings have been extended in recent years by results that indicate the significance of spermatozoal RNA during oocyte fertilization (Ostermeier *et al.*, 2004) and which revealed specific mRNA patterns that correlate with male fertility/infertility (Wang *et al.*, 2004; Garrido *et al.*, 2009; Lalancette *et al.*, 2009; Garcia-Herrero *et al.*, 2010) or sperm function (Lambard *et al.*, 2004; Platts *et al.*, 2007).

With the need of highly purified spermatozoal RNA for downstream applications such as PCR or microarray analysis arises the essential requirement to eliminate contaminating DNA from the RNA samples prior to analysis. Specific to spermatozoal RNA is the inherent problem of an unusual DNA:RNA ratio that differs substantially from that of somatic cells. Being somewhat different between species, descriptions of spermatozoal RNA content vary between 0.18 fg/sperm (cattle; Gilbert *et al.*, 2007), 5 fg/sperm (domestic swine; Yang *et al.*, 2009) and 15–400 fg/sperm in the human (Miller *et al.*, 2005; Goodrich *et al.*, 2007; Lalancette *et al.*, 2009). A calculated 3.5 pg DNA/sperm (3.2E9 bp [genome size] * 660 Da/bp [average mol. weight of a basepair] * 1.66E-27 kg/Da [weight of one standard unit]) indicates a 10- to 100-fold excess of DNA over RNA in spermatozoa, in contrast to a roughly 10-fold excess of RNA (10–30 pg/cell) over DNA in somatic cells. Hence, RNA extraction protocols for spermatozoa need to be specifically tailored to address this issue by giving a strong focus on the removal of genomic DNA. Established extraction protocols for spermatozoal RNA can be categorized into phase-separation/precipitation methods (Ostermeier *et al.*, 2002; Lambard *et al.*, 2004; Wang *et al.*, 2004; Garrido *et al.*, 2009; Nguyen *et al.*, 2009; Garcia-Herrero *et al.*, 2010), affinity purification columns (Ostermeier *et al.*, 2005; Goodrich *et al.*, 2007; Platts *et al.*, 2007; Lalancette *et al.*, 2009; Yang *et al.*, 2009) or combinations thereof (Gilbert *et al.*, 2007; Linschooten *et al.*, 2009; Das *et al.*, 2010). Furthermore, many of these protocols employ an additional DNase I digestion step in order to remove residual genomic DNA or utilize heated extraction, the latter having been shown to alter the electrophoretic RNA pattern (Gilbert *et al.*, 2007) or shorten transcript length (Bissonnette *et al.*, 2009). The double-column protocol presented in this study results (when starting with a maximum of 2×10^7 sperm) in a highly purified total RNA fraction which avoids the use of DNase I that is frequently contaminated with residual RNase activity (Goodrich *et al.*, 2007) and that might be inhibitory in downstream applications.

Using this novel protocol, the ejaculate RNA uncovered a distinct microelectrophoretic pattern consisting of several bands together with two prominent bands. In the somatic context, these two bands have been shown several decades ago to reflect 18S and 28S rRNA (Loening, 1967). Additional bands were evident, possibly pertaining to mitochondrial rRNA (16S and 12S rRNA; Villegas *et al.*, 2002) or highly abundant transcripts. This unexpected pattern contradicts existing reports claiming the absence of ribosomal RNAs in human spermatozoa (Ostermeier *et al.*, 2002; Linschooten *et al.*, 2009; Yang *et al.*,

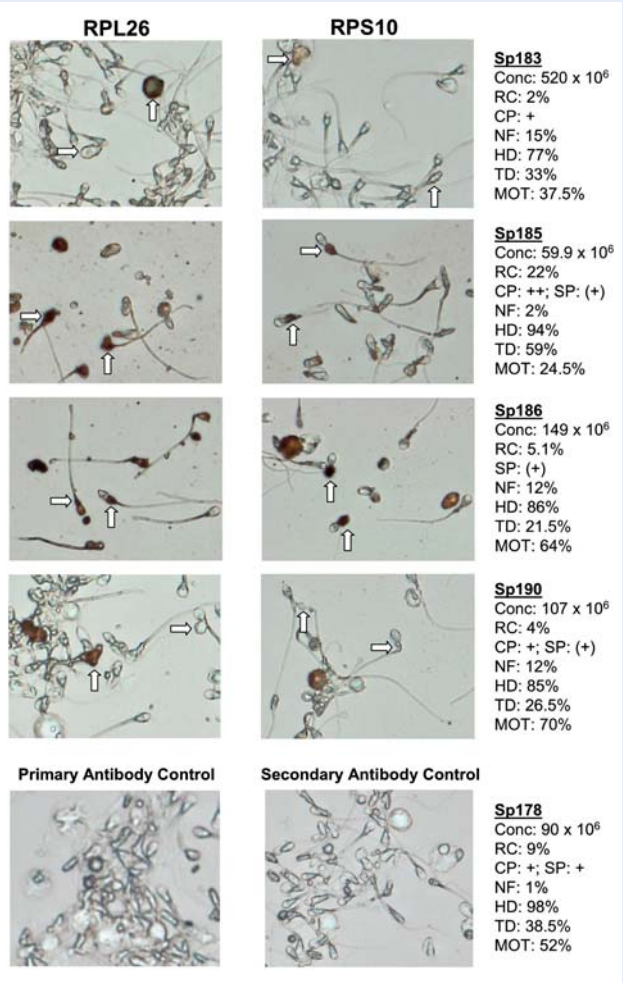

Figure 6 Immunohistochemical analysis of normo- and teratozoospermic ejaculates for the presence of large and small ribosomal subunit proteins (RPL26 and RPS10). While normozoospermic ejaculates Sp183/Sp190 displayed exclusive staining in somatic round cells and not in malformed spermatozoa (white arrows), teratozoospermic sample Sp185 and normozoospermic sample Sp186 showed intense staining for both ribosomal proteins in spermatozoa with head/tail defects or extensive midpiece cytoplasm (white arrows). Specificity of the signals was evaluated with primary and secondary antibody controls (Sp178). Magnification: 200×. Abbreviations of spermiogram data: Conc, concentration [sperm/ml]; RC, round cell quantity (as analyzed by cytological staining); CP, amount of cytoplasm in spermatozoa; SP, amount of round spermatogenic cells (as analyzed by cytological staining); NF, normal forms quantity; HD, head defects; TD, tail defects; MOT, motility (a + b category).

2009; Das *et al*., 2010). However, other reports of ribosomal RNA in human spermatozoa (Betlach and Erickson, 1976; Gur and Breitbart, 2006) motivate to revisit this topic. Descriptions of 18S and 28S rRNA bands in the microelectrophoretic traces of density gradient-purified bovine spermatozoa (Gilbert *et al*., 2007) might point to the fact that the sensitivity of the electrophoretic system is crucial for the detection of spermatozoal rRNA. Furthermore, pretreatment of ejaculates in order to eliminate somatic cells such as 'somatic lysis' (Ostermeier *et al*., 2002; Ostermeier *et al*., 2005; Goodrich *et al*., 2007; Lalancette *et al*., 2009; Linschooten *et al*., 2009), density gradient centrifugation (Gilbert *et al*., 2007; Bissonnette *et al*., 2009; Das *et al*., 2010) or swim-up (Yang *et al*., 2009; Garcia-Herrero *et al*., 2010) is prone to deliver diverging results.

Our results from comparing ejaculates with very low round cell contamination to those that have high round cell quantities, and the results from obtaining a highly purified spermatozoal fraction by density gradient centrifugation, indicate clearly that the round cell quantity correlates with the presence of the 28S rRNA band. Contrasting this, the 18S rRNA peak is observed in ejaculates irrespective of round cell content and seems to be an inherent characteristic of purified spermatozoa, with the 28S/18S rRNA ratio estimated to be ~0.1 by qPCR. In the presence of a somatic compartment as in testicular samples, the 28S/18S rRNA ratio is significantly higher than in ejaculates, pointing to an enrichment of 28S rRNA in somatic cells.

Although not evaluated for 28S rRNA, Gur and Breitbart (2006) showed that cytoplasmic 18S rRNA is predominantly associated with a monosomal fraction, indicating that cytoplasmic ribosomes are present, but not active in spermatozoa. Our transmission electron microscopy (TEM) evaluation of cytoplasmic ribosomes in spermatozoa support these findings by showing a significant number of electron-dense ribosomal structures, mostly irregularly dispersed and giving the impression of monosomes, while some structures displayed a polysomal-like appearance. It cannot be ruled out that the latter is due to stochastical dispersion of monosomes giving a polysomal impression.

These observations are in conflict with the generally accepted hallmark feature of spermatozoa lacking ribosomal RNAs (Miller *et al*., 2005). Our TEM and immunohistochemical data clearly support the existence of cytoplasmic ribosomes in ejaculate spermatozoa. It is obvious that the amount of isolated rRNA correlates with the overall cytoplasmic quantity of the spermatozoa in the individual ejaculates. Using a prefixation protocol, we found a high number of spermatozoa with considerable cytoplasm similar to the 50% described in motile fractions by Cooper *et al*. (2004). A further interesting aspect concerning the detection of ribosomal RNA is, besides the sensitivity of the electrophoretic system leading to discrete 18S and 28S rRNA bands (Gilbert *et al*., 2007), the amount of contaminating DNA. One round of column amplification was not sufficient enough to remove the complete genomic DNA, resulting in all rRNA bands being obscured (compare Fig. 1). However, the reason for absence of 28S rRNA in purified spermatozoa remains to be resolved. Experimental degradation of the 28S rRNA in our samples seems unlikely as the profiles obtained from different round cell quantities are highly similar and one would expect additional bands of 28S rRNA degradation products. Although there was some heterogeneity between different ejaculates with respect to the immunohistochemical detection of two proteins pertaining to the small and large ribosomal subunit, spermatozoal cytoplasm was always positive for both proteins. This suggests that at least these two, but not necessarily all, protein components of the ribosomes may be present in spermatozoa. In light of lacking 28S rRNA, which can be considered as the large subunits backbone, it seems likely that spermatozoal cytoplasmic ribosomes are not functionally assembled, in contrast to their mitochondrial counterpart which exhibit full translational activity (Gur and Breitbart, 2006). In the absence of functional 80S cytoplasmic

ribosomes, it is possible that ribosomal RNAs of the large subunit undergo non-functional RNA decay in the exosome (Cole *et al.*, 2009) and are therefore depleted in the isolated total RNA pool. Similar to paternal mitochondria and paternal mRNA species such as protamine-1, protamine-2 and GAPDH which are subjected to selective decay within the oocyte (Cummins, 2000; Ziyyat and Lefevre, 2001; Hayashi *et al.*, 2003), paternal cytoplasmic ribosomes might be kept in a disassembled state ensuring that no post-fertilization translation of hazardous transcripts takes place.

For those ejaculates for which we had additional data with respect to fertilization outcome (all in Fig. 2), we observed in some cases with negative pregnancy outcome quite prominent 18S rRNA bands (such as FCH_22, FCH_30, FCH_13; compare Fig. 2), pointing to a potential influence of paternal rRNA transcripts on oocyte fertilization. In the same lines, a study from Lalancette *et al.* (2008) comparing bulls with high and low return rate found an increased abundance of a ribosomal RNA in bulls with low return rates. We queried the sequence of this rRNA and found it to be 99% identical (nucleotides 165–579) to the human 18S rRNA (NR_003286.1), although it was initially declared as a mitochondrial rRNA (Accession AB098876.1). Hence, an increased abundance of 18S rRNA in human spermatozoa could have a similar effect on fertilization outcome.

Future studies should examine the exact structural features of spermatozoal ribosomes in more detail, such as scanning electron microscopy to analyze ribosomal subunits, and correlate ribosomal integrity with spermatozoal quality criteria and possible effects on fertilization/pregnancy outcome. During the review process of this paper, we became aware of a study from Payton *et al.* (2010). Similar to our findings on the male side, the authors describe an unusual 28S/18S rRNA ratio in bovine oocytes, which is not evident in the presence of somatic cumulus cells. These results together with our own strongly point to a general gamete-specific reduction in 28S rRNA quantity.

Supplementary data

Supplementary data are available at http://molehr.oxfordjournals.org/.

Authors' roles

H.C.O. conducted the majority of experiments and made the figures. W.S. was involved in the study design. H.J. conducted the TEM evaluation of ribosomes. V.B. isolated semen samples from the fertility clinic. A.N.S. wrote the manuscript and structured the study.

Acknowledgements

Financial support of this work from grant Sp721/1-3 of the German Research Foundation to ANS and HCO is gratefully acknowledged. We thank Prof. Christiane Kirchhoff for fruitful discussions.

Funding

Financial support of this work is obtained from grant Sp721/1-3 of the German Research Foundation.

References

Avendano C, Franchi A, Jones E, Oehninger S. Pregnancy-specific β-1-glycoprotein 1 and human leukocyte antigen-E mRNA in human sperm: differential expression in fertile and infertile men and evidence of a possible functional role during early development. *Hum Reprod* 2009;**24**:270–277.

Betlach CJ, Erickson RP. 28 s and 18 s ribonucleic acid from mammalian spermatozoa. *J Exp Zool* 1976;**198**:49–55.

Bissonnette N, Levesque-Sergerie JP, Thibault C, Boissonneault G. Spermatozoal transcriptome profiling for bull sperm motility a potential tool to evaluate semen quality. *Reproduction* 2009; **138**:65–80.

Cole SE, LaRiviere FJ, Merrikh CN, Moore MJ. A convergence of rRNA and mRNA quality control pathways revealed by mechanistic analysis of nonfunctional rRNA decay. *Mol Cell* 2009;**34**:440–450.

Cooper TG, Yeung CH, Fetic S, Sobhani A, Nieschlag E. Cytoplasmic droplets are normal structures of human sperm but are not well preserved by routine procedures for assessing sperm morphology. *Hum Reprod* 2004;**19**:2283–2288.

Cummins JM. Fertilization and elimination of the paternal mitochondrial genome. *Hum Reprod* 2000;**15** (Suppl. 2): 92–101.

Dadoune JP, Siffroi JP, Alfonsi MF. Transcription in haploid male germ cells. *Int Rev Cytol* 2004;**237**:1–56.

Dadoune JP, Pawlak A, Alfonsi MF, Siffroi JP. Identification of transcripts by macroarrays, RT-PCR and in situ hybridization in human ejaculate spermatozoa. *Mol Hum Reprod* 2005;**11**:133–140.

Das PJ, Paria N, Gustafson-Seabury A, Vishnoi M, Chaki SP, Love CC, Varner DD, Chowdhary BP, Raudsepp T. Total RNA isolation from stallion sperm and testis biopsies. *Theriogenology* 2010; **74**:1099–1106e2.

Feig C, Kirchhoff C, Ivell R, Naether O, Schulze W, Spiess AN. A new paradigm for profiling testicular gene expression during normal and disturbed human spermatogenesis. *Mol Hum Reprod* 2007;**13**:33–43.

Garcia-Herrero S, Meseguer M, Martinez-Conejero JA, Remohi J, Pellicer A, Garrido N. The transcriptome of spermatozoa used in homologous intrauterine insemination varies considerably between samples that achieve pregnancy and those that do not. *Fertil Steril* 2010;**94**:1360–1373.

Garrido N, Martinez-Conejero JA, Jauregui J, Horcajadas JA, Simon C, Remohi J, Meseguer M. Microarray analysis in sperm from fertile and infertile men without basic sperm analysis abnormalities reveals a significantly different transcriptome. *Fertil Steril* 2009;**91**:1307–1310.

Gilbert I, Bissonnette N, Boissonneault G, Vallee M, Robert C. A molecular analysis of the population of mRNA in bovine spermatozoa. *Reproduction* 2007;**133**:1073–1086.

Giordano R, Magnano AR, Zaccagnini G, Pittoggi C, Moscufo N, Lorenzini R, Spadafora C. Reverse transcriptase activity in mature spermatozoa of mouse. *J Cell Biol* 2000;**148**:1107–1113.

Goodrich R, Johnson G, Krawetz SA. The preparation of human spermatozoal RNA for clinical analysis. *Arch Androl* 2007;**53**:161–167.

Grunewald S, Paasch U, Glander HJ, Anderegg U. Mature human spermatozoa do not transcribe novel RNA. *Andrologia* 2005;**37**: 69–71.

Gur Y, Breitbart H. Mammalian sperm translate nuclear-encoded proteins by mitochondrial-type ribosomes. *Genes Dev* 2006;**20**:411–416.

Hayashi S, Yang J, Christenson L, Yanagimachi R, Hecht NB. Mouse preimplantation embryos developed from oocytes injected with round spermatids or spermatozoa have similar but distinct patterns of early messenger RNA expression. *Biol Reprod* 2003;**69**:1170–1176.

Krawetz SA. Paternal contribution: new insights and future challenges. *Nat Rev Genet* 2005;**6**:633–642.

Kumar G, Patel D, Naz RK. c-MYC mRNA is present in human sperm cells. *Cell Mol Biol Res* 1993;**39**:111–117.

Lalancette C, Thibault C, Bachand I, Caron N, Bissonnette N. Transcriptome analysis of bull semen with extreme nonreturn rate: use of suppression-subtractive hybridization to identify functional markers for fertility. *Biol Reprod* 2008;**78**:618–635.

Lalancette C, Platts AE, Johnson GD, Emery BR, Carrell DT, Krawetz SA. Identification of human sperm transcripts as candidate markers of male fertility. *J Mol Med* 2009;**87**:735–748.

Lambard S, Galeraud-Denis I, Bouraima H, Bourguiba S, Chocat A, Carreau S. Expression of aromatase in human ejaculated spermatozoa: a putative marker of motility. *Mol Hum Reprod* 2003; **9**:117–124.

Lambard S, Galeraud-Denis I, Martin G, Levy R, Chocat A, Carreau S. Analysis and significance of mRNA in human ejaculated sperm from normozoospermic donors: relationship to sperm motility and capacitation. *Mol Hum Reprod* 2004;**10**:535–541.

Linschooten JO, Van Schooten FJ, Baumgartner A, Cemeli E, Van Delft J, Anderson D, Godschalk RW. Use of spermatozoal mRNA profiles to study gene-environment interactions in human germ cells. *Mutat Res* 2009;**667**:70–76.

Loening UE. The fractionation of high-molecular-weight ribonucleic acid by polyacrylamide-gel electrophoresis. *Biochem J* 1967;**102**:251–257.

Miller D, Briggs D, Snowden H, Hamlington J, Rollinson S, Lilford R, Krawetz SA. A complex population of RNAs exists in human ejaculate spermatozoa: implications for understanding molecular aspects of spermiogenesis. *Gene* 1999;**237**:385–392.

Miller D, Ostermeier GC, Krawetz SA. The controversy, potential and roles of spermatozoal RNA. *Trends Mol Med* 2005;**11**:156–163.

Miller D, Brinkworth M, Iles D. Paternal DNA packaging in spermatozoa: more than the sum of its parts? DNA, histones, protamines and epigenetics. *Reproduction* 2010;**139**:287–301.

Nguyen MT, Delaney DP, Kolon TF. Gene expression alterations in cryptorchid males using spermatozoal microarray analysis. *Fertil Steril* 2009;**92**:182–187.

Ostermeier GC, Dix DJ, Miller D, Khatri P, Krawetz SA. Spermatozoal RNA profiles of normal fertile men. *Lancet* 2002;**360**:772–777.

Ostermeier GC, Miller D, Huntriss JD, Diamond MP, Krawetz SA. Reproductive biology: delivering spermatozoan RNA to the oocyte. *Nature* 2004;**429**:154.

Ostermeier GC, Goodrich RJ, Diamond MP, Dix DJ, Krawetz SA. Toward using stable spermatozoal RNAs for prognostic assessment of male factor fertility. *Fertil Steril* 2005;**83**:1687–1694.

Payton RR, Rispoli LA, Edwards JL. General features of certain RNA populations from gametes and cumulus cells. *J Reprod Dev* 2010; **56**:583–592.

Pessot CA, Brito M, Figueroa J, Concha II, Yanez A, Burzio LO. Presence of RNA in the sperm nucleus. *Biochem Biophys Res Commun* 1989; **158**:272–278.

Pfaffl MW. A new mathematical model for relative quantification in real-time RT-PCR. *Nucleic Acids Res* 2001;**29**:e45.

Pittoggi C, Beraldi R, Sciamanna I, Barberi L, Giordano R, Magnano AR, Torosantucci L, Pescarmona E, Spadafora C. Generation of biologically active retro-genes upon interaction of mouse spermatozoa with exogenous DNA. *Mol Reprod Dev* 2006;**73**:1239–1246.

Platts AE, Dix DJ, Chemes HE, Thompson KE, Goodrich R, Rockett JC, Rawe VY, Quintana S, Diamond MP, Strader LF *et al.* Success and failure in human spermatogenesis as revealed by teratozoospermic RNAs. *Hum Mol Genet* 2007;**16**:763–773.

Rassoulzadegan M, Grandjean V, Gounon P, Cuzin F. Inheritance of an epigenetic change in the mouse: a new role for RNA. *Biochem Soc Trans* 2007;**35**:623–625.

Steger K, Fink L, Failing K, Bohle RM, Kliesch S, Weidner W, Bergmann M. Decreased protamine-1 transcript levels in testes from infertile men. *Mol Hum Reprod* 2003;**9**:331–336.

Villegas J, Araya P, Bustos-Obregon E, Burzio LO. Localization of the 16S mitochondrial rRNA in the nucleus of mammalian spermatogenic cells. *Mol Hum Reprod* 2002;**8**:977–983.

Wang H, Zhou Z, Xu M, Li J, Xiao J, Xu ZY, Sha J. A spermatogenesis-related gene expression profile in human spermatozoa and its potential clinical applications. *J Mol Med* 2004; **82**:317–324.

Wykes SM, Visscher DW, Krawetz SA. Haploid transcripts persist in mature human spermatozoa. *Mol Hum Reprod* 1997;**3**:15–19.

Yang CC, Lin YS, Hsu CC, Wu SC, Lin EC, Cheng WT. Identification and sequencing of remnant messenger RNAs found in domestic swine (Sus scrofa) fresh ejaculated spermatozoa. *Anim Reprod Sci* 2009; **113**:143–155.

Ziyyat A, Lefevre A. Differential gene expression in pre-implantation embryos from mouse oocytes injected with round spermatids or spermatozoa. *Hum Reprod* 2001;**16**:1449–1456.